Archaeointensity Determinations from Finland, Estonia, and Italy

Fabio Donadini[1,2] *and Lauri J. Pesonen*[1]

[1] Division of Geophysics, University of Helsinki, Gustav Hällströmin Katu 2, 00014 Helsinki, Finland

[2] Scripps Institution of Oceanography, University of California at San Diego, 9500 Gilman Drive, La Jolla, CA 92093-0225, USA

Abstract

In this paper we summarize a palaeointensity study performed on different archaeological collections from Finland and Estonia, as well as on a collection of stamped Roman bricks (AD 110–123). The collection from Finland represents a set of baked clays and bricks, dated with calibrated ^{14}C or by historical methods (Nurmes church brick, AD 1893) and covering a period between 5080 BC and AD 1893. The collection from Estonia consists of different potteries, tiles, and bricks, dated between the 5th century and AD 1770. The reliable results were compared with the Finnish archaeointensity master curve and with the relative intensity curves obtained from Scandinavian lake sediments, and show in general a good agreement. The result from the stamped Roman brick agrees with other palaeointensity data from France and Italy covering the same period.

1.   *Introduction*

The Earth's magnetic field (EMF) varies its intensity and direction during time. Studies aiming to define the EMF characteristics at a particular place and time are of particular interest to understand the present behaviour as well as future changes of our planet. Some authors have pointed out the possibility of an imminent reversal (e.g. *Hulot et al.*, 2002; *Constable and Korte*, 2006); others see a link between the sudden variation in EMF directions and intensities (so called archaeomagnetic jerks) and climate changes (*Gallet et al.*, 2005). Moreover, the importance of EMF studies in the past time is underlined by the fact that its outcome constitutes the raw material to construct theoretical models (e.g. *Korte and Constable*, 2005).

When looking at the archaeointensity data available worldwide (e.g. *Donadini et al.*, 2006) one notices that the geographical distribution of the data is centered on low to moderate latitudes of the Northern hemisphere. In this sense, Finland (60–70° N) represents a unique possibility to extend the archaeomagnetic research to higher latitudes. One of the main aims of this study was to improve the North European archaeointensity master curve with new samples from Finland and Estonia.

The new measurements are compared with the Scandinavian master curve compiled by *Pesonen et al.* (1995), *Riisager et al.* (2003), *Gram-Jensen et al.* (2000), *Donadini et al*. (2007). The curves are also compared with the output for the CALS7k model of (*Korte and Constable*, 2005) produced for the locality of Kajaani (64.2° N – 27.3° E), representative central point for Finland. Scandinavia is also rich of well dated lake sediments (*Ojala and Saarinen,* 2002, *Snowball and Sandgren,* 2002), and so it is worthwhile to compare the output of the new archaeointensity measurements with those of lake sediments, particularly with the ones that are well dated using calibrated radiocarbon (^{14}C) or varve counting.

Stamped archaeological objects represents an opportunity to associate accurately the geomagnetic field intensity value with a particular age. In this paper the measurement from two stamped archaeological objects (Roman bricks and Estonian tiles) are presented.

2.   Sample selection

Fig. 1 shows the location of the collected samples, the key number referring to the numbers reported in Tables 1, 2, and 3.

The samples were collected from different museums or from private persons. In general we obtained dated potteries or bricks, which have accurate dating such as calibrated radiocarbon ages or stamps.

In particular, the Hela dataset (Fig. 1, key no. 1–5) is a collection of baked clays from high latitudes (63–67°N), and are of particular interest for the global intensity models, which lack data from high latitudes. These materials were dated using calibrated ^{14}C at the Dating Laboratory of the University of Helsinki, and have ages spanning over the period between 5100 BC and 615 BC (Jungner, 2004, pers. comm.). This interval covers a part of the Scandinavian master curve that is poor in data. Additionally, a brick from the Church of Nurmes (AD 1893, Fig.1, key no. 6) was investigated.

A set of Estonian potteries (Fig.1, key no. 7–9, 11, 13) was donated by Professor Valter Lang, from the Department of Archaeology of the University of Tartu. The ages of these samples span between AD 0 and 12th century AD, with particular focus on the 5th century AD, when the field intensity appears to reach a maximum in Finland (*Pesonen et al.,* 1995). Professor Lang also gave two tile fragments, both stamped, with ages of AD 1550 (Fig. 1, key no. 12) and 1770 (Fig. 1, key no. 10), respectively. One brick from the Jaani Cathedral located in Tartu (Fig. 1, key no. 14), and dated late 13th century AD, was given by MSc Tiiu Elbra.

Additionally, three stamped Roman bricks that were donated by Professor Päivi Setälä (University of Helsinki) and are dated AD 110–120 (Fig. 2).
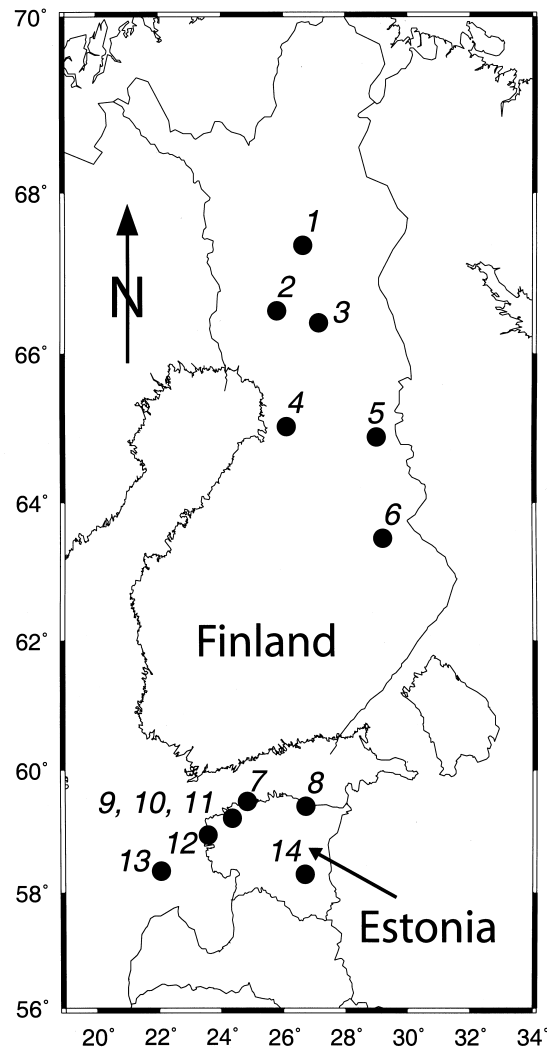
Fig. 1. Location of the archaeological samples from Scandinavia. Two degrees on the map correspond to 220 km.

3.   *Methodology*

Magnetic measurements were carried out at the Solid Earth Laboratory of the University of Helsinki using an AGICO spinner magnetometer (JR6a).

To define the magnetic minerals that define the main remanence carriers, high temperature susceptibility curves in conjunction with hysteresis analyses were performed using a AGICO KLY3 kappabridge, and a Micromag Vibrating Sample Magnetometer (Princeton measurements Co.), respectively.

Palaeointensity measurements were carried out using the Thellier technique modified after *Coe* (1967), with additional alteration checks (*Coe,* 1967) and tail checks (e.g. *Riisager and Riisager,* 2001). All specimens were oriented in the oven so that their Characteristic Remanent Magnetization (ChRM) was aligned with the laboratory field (B$_{lab}$). This strategy avoids problems related to the fabric anisotropy effects, which might be considerable in potteries and bricks (e.g. *Pesonen et al.,* 1995).

Table 1. Main characteristics of the magnetic properties of the material studied. The sample type is denoted as pottery (pot.), brick (br.), or tile (ti.). Key denotes the numbers given in Fig. 1. T_C gives the Curie temperature defined by thermomagnetic analyses. Hysteresis parameters are defined as follows: M_S [mAm^2/kg] is the saturation magnetization, M_{RS} [mAm^2/kg] is the saturation remanent magnetization, H_C [mT] is the coercive field, H_{CR} [mT] is the coercivity of remanence.

Sample	type	key	T_C	min. change	M_{RS}	M_S	H_C	H_{CR}	M_S / M_{RS}	H_{CR} / H_C
			Finnish potteries and bricks							
Hela39	pot.	1	370; 550; 630	moderate	308.3	1150	18.0	30.9	0.27	1.72
Rova	pot.	2	440; 570	moderate	191.2	644.6	19.3	31.0	0.30	1.60
Hela20	pot.	3	435; 580	signif.	0.007	0.041	8.5	25.0	0.17	2.94
Hela37	pot.	3	350; 570; 625	signif.	0.3	2.2	9.7	29.4	0.12	3.02
Hela42	pot.	4	390; 560	moderate	73.7	233	13.6	25.9	0.32	1.90
Hela138	pot.	4	340; 563	signif.	10.6	59.5	6.8	18.4	0.18	2.71
Hela146	pot.	4	370; 560; 625	signif.	12.6	88.2	5.0	19.8	0.14	3.99
Hela148	pot.	4	350; 555	signif.	154.9	670.8	7.5	17.4	0.23	2.34
Nurmes	br.	6	330; 550	signif.	114.9	278.9	10.0	17.3	0.41	1.73
			Estonian potteries, bricks, and tiles							
VI1	pot.	7	350; 580	signif.	66.6	192.1	16.1	33.4	0.35	2.08
VI2	pot.	7	350; 580; 680	insignif.	61.5	152.4	16.8	28.6	0.40	1.70
VI3	pot.	7	160; 420; 580	signif.	64.4	222.3	9.2	19.6	0.29	2.13
PD1	pot.	8	150; 560; 680	signif.	141.1	516	7.8	15.7	0.27	2.01
PD2	pot.	8	580	insignif.	11.8	45	8.7	30.2	0.26	3.47
LT1	pot.	9			3.2	16.6	5.7	18.6	0.19	3.26
LT2	pot.	9	350; 540	insignif.	410.5	996.8	21.5	40.2	0.41	1.87
TA1	ti.	10	580	signif.	29.4	182.5	5.4	37.8	0.16	7.05
MU1	pot.	11	150; 350; 560	signif.	70.1	295.2	7.5	25.2	0.24	3.38
MU2	pot.	11	350; 580	insignif.	192.9	953.2	10.1	26.5	0.20	2.64
PJ1	pot.	13	350; 560	insignif.	508.8	1281	14.8	30.0	0.40	2.03
PJ2	pot.	13	350; 540	signif.	23.1	170.2	2.3	15.6	0.14	6.76
TB	br.	14	380; 540; 680	insignif.	4.4	16.4	9.3	19.0	0.27	2.04
			Roman brick							
RB01	br.		320; 540	insignif.	10.6	56.6	3.3	19.7	0.19	5.96
RB02	br.		270; 540; 580	signif.	9.3	36	9.6	34.2	0.26	3.56
RB03	br.		390; 580	insignif.	68.5	85.3	8.6	13.9	0.80	1.62

Table 2. Archaeointensity results of various archaeological collections from Finland (F), Estonia (E), and Italy (I). Key relates to the number in Fig. 1. Dat. indicates the method used to define the age: calibrated ^{14}C (C), archaeological (A), historical (H), or annual stamps (S). Results indicate the palaeofield B_a and its standard deviation σB_a [μT], the temperature interval used to define the slope on the Arai diagram ($T_{min} - T_{max}$), the quality factor q, and the NRM fraction f.

Sample	location	key	age	σ_{age}	Dat	B_a	σB_a	T_{min}	T_{max}	f	q
Hela146	Ylikiiminki, F	4	-5080	150	C		rejected				
Hela148	Ylikiiminki, F	4	-4635	95	C		rejected				
Hela42	Ylikiiminki, F	4	-4625	105	C	41.7	1.2	200	535	0.71	20.60
Hela37	Kemijärvi, F	3	-1465	65	C		rejected				
Hela20	Kemijärvi, F	3	-1300	100	C	55.5	1.4	20	510	0.66	23.50
Hela20-1b						54.2	4.0	230	535	0.83	9.89
Hela97	Suomussalmi, F	5	-670	150	C	60.7	2.0	100	350	0.42	9.70
Hela39	Sodankylä, F	1	-615	95	C		rejected				
Rova	Rovaniemi, F	2			C		rejected				
MU1-1a	Muskylä, E	11	0	100	A	76.6	3.4	100	580	0.96	19.20
MU2-1a						79.3	6.5	150	470	0.60	6.50
LT1-1a						27.4	1.9	20	580	1.00	13.00
LT2-1a	Läätsä, E	9	late 5th c.		A		rejected				
LT2-1b						81.7	7.6	20	500	0.74	7.61
PJ1-1a	Paju, E	13	5th c.		A	83.4	7.9	200	500	0.66	6.10
PJ2-1a						38.0	1.3	200	500	0.54	13.00
VI1-1a							rejected				
VI1-1b							rejected				
VI1-1c							rejected				
VI2-1a	Viimsi, E	7	late 5th c.		A	94.4	8.1	320	580	0.88	7.60
VI2-1b							rejected				
VI3-1a						86.5	4.1	100	500	0.58	10.20
VI3-1b						81.0	2.5	100	500	0.59	16.10
PD1-1a	Pada, E	8	12th c		A	57.3	2.1	350	500	0.44	9.00
PD2-1a						53.4	2.8	100	470	0.62	10.40
TB1-1a	Tartu, E	14	1400		H	68.1	1.6	20	510	0.82	28.00
TB1-1b						68.8	1.3	20	380	0.58	21.00
HA1-1a	Haapsalu, E	12	1550	5	S	50.8	2.5	200	580	0.82	13.60
TA1-1a	Tallin, E	10	1770	5	S	55.8	3.5	150	500	0.47	6.40
NU1-1a						49.7	3.6	100	510	0.83	9.70
NU1-1b	Nurmes, F	6	1893		H	57.5	5.5	250	460	0.59	5.00
NU1-7a						41.2	1.3	320	570	0.52	13.50
RB01						63.6	3.6	100	550	0.84	13.30
RB02a							rejected				
RB02b	Rome, I		110		S		rejected				
RB03a						63.5	0.9	100	400	0.91	49.40
RB03b						72.1	2.1	20	360	0.78	22.40

Fig. 2. Roman brick donated by Prof. Päivi Setälä, and dated AD 123. (Photograph: Kari A. Kinnunen, Geological Survey of Finland).

4.   Rock magnetic measurements

The rock magnetic measurements consisting of high temperature susceptibility curves as well as hysteresis analysis are presented in Table 1. Notice that no rock magnetic investigation was possible for specimen Hela97 and HA1-1a (key no. 5 and 12) due to the small size of the specimens. Most samples show complex thermo-magnetic curves (Fig. 3). In general the main magnetic carrier is titanomagnetite (Curie temperature T_C about 540–580° C). Several specimens also indicate the presence of maghemite (about 350° C), and hematite (about 680° C), and in two specimens goethite (about 150° C) was also detected. In addition, many of the thermomagnetic curves show irreversible character when heated in air, suggesting that chemical alteration has taken place.

The complex mineralogy is also reflected in the hysteresis loops (Fig. 4), which are in many cases wasp-waisted, and indicate the presence of both high and low coercivity phases.

The hysteresis measurements show that the grains lie mainly in the PSD area of the Day plot (Fig. 5; *Day et al.,* 1977).

Fig. 3. Thermomagnetic curves (susceptibility versus temperature) for representative samples from Table 1. The susceptibility is normalized by its maximum value. Black (gray) dots denote the heating (cooling) curves.
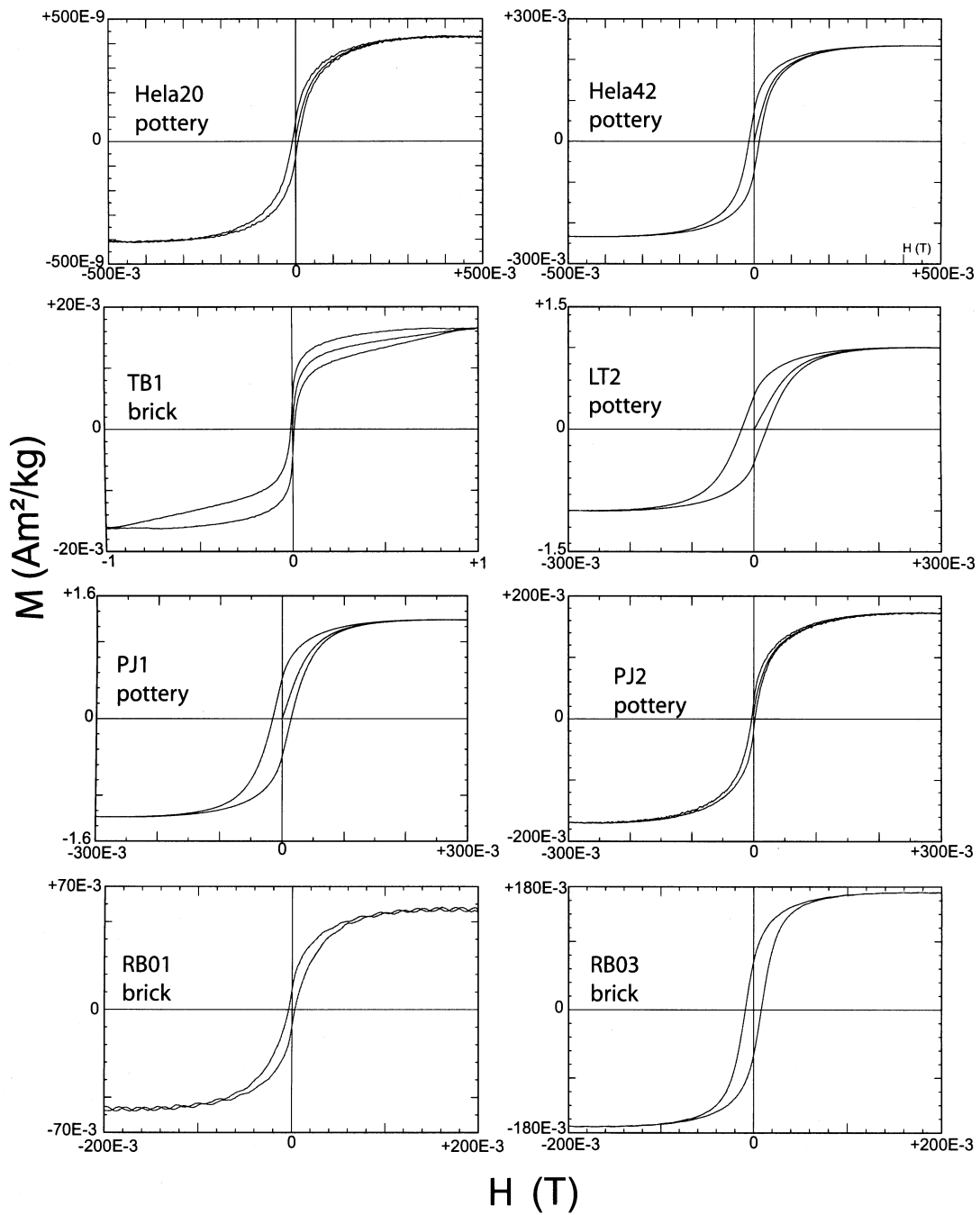
Fig. 4. Hysteresis loops for representative samples given in Table 1. The mass normalized magnetization (M) is plotted as a function of the applied field (H).
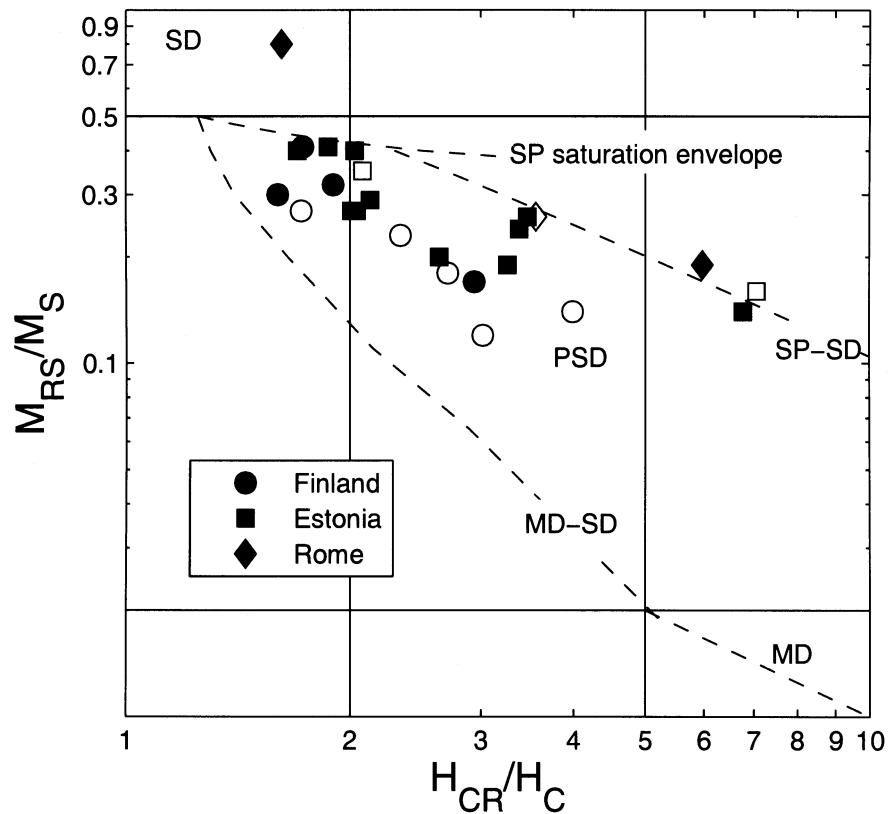
Fig. 5. Hysteresis data presented as a Day plot. Different symbols represent different regions. Open (closed) symbols display rejected (accepted) specimens.

5.   Palaeointensity results

The palaeointensity results are summarized in Table 2. Examples of palaeointensity results are displayed in Fig. 6 and Fig. 7. In general, when more than one specimen was measured, the agreement between single results is good. However, in the cases of Läätsä and Paju (sites 9 and 13) we notice discrepancies. Läätsä results are about 45 % offset, and Paju results about 40 % (see also Fig. 7). These samples were not accounted in the calculation of the mean palaeointensity values (Table 3). A possible explanation to this discrepancy is that the samples show different thermomagnetic characteristics: the lower palointensities were obtained from the samples with larger variability between heating and cooling curve. The hysteresis loops (Fig. 3) clearly shows that the features of PJ1 loop are typical of SD like granulometry, whereas the thin loop observed for PJ2 is more typical for non ideal MD grain assemblages.
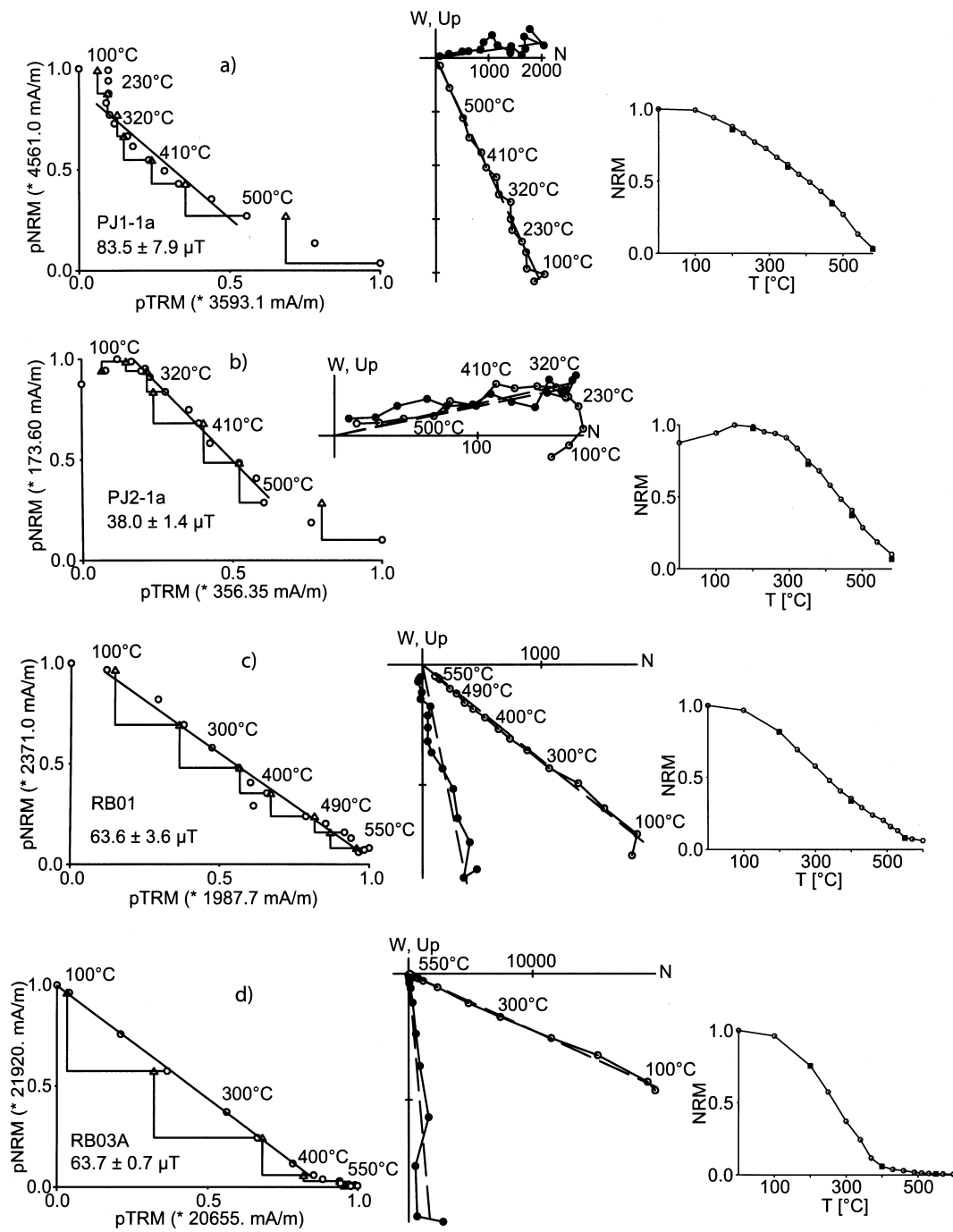
Fig. 6 Examples of archaeointensity results: Arai plot (left), Zijderveld plot (middle), and intensity decay plot (right). Samples Hela20 (a) and Hela97 (b) are Finnish potteries, MU1-1a (c) Estonian pottery, and TB1-1a (d) an Estonian brick.
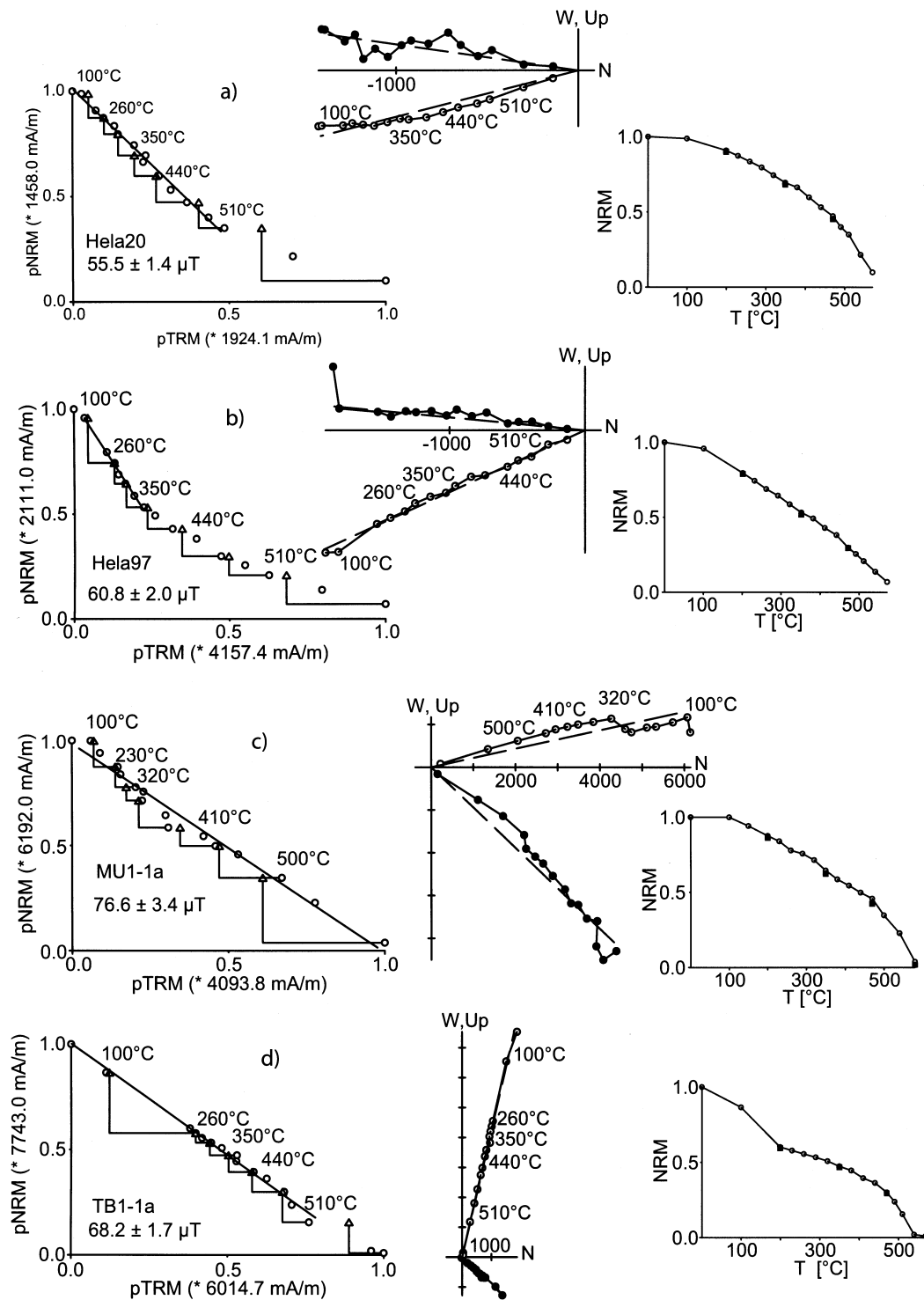
Fig. 7. Examples of archaeointensity results: Arai plot (left), Zijderveld plot (middle), and intensity decay plot (right). Samples PJ1-1a (a) and PJ2-1a (b) are Estonian potteries, RB01 (c) and RB03a (d) are stamped Roman bricks.

Table 3. Mean archaeointensity values B_a [μT] and VADM [10^{22} Am^2], and associated standard deviations obtained from the various collections. Key represents the number shown in Fig. 1, age and σ_{age} denote the dating of the artifacts and their standard deviation, in years AD (positive) and BC (negative). The type of the specimen is denoted as pottery (pot.), brick (br.), or tile (ti.); λ_g represents the site latitude, N the number of specimens measured.

Location	type	key	N	age	σ_{age}	B_a	σB_a	λ_g	VADM	σVADM
Ylikiiminki, F	pot.	4	1	-4625	105	41.7	1.2	65.0	5.8	0.2
Kemijärvi, F	pot.	3	2	-1300	100	54.8	0.9	66.4	7.5	0.1
Suomussalmi, F	pot.	5	1	-670	150	60.7	2.0	64.9	8.4	0.3
Muskylä, E	pot.	11	2	0	100	77.9	1.9	59.2	11.2	0.2
Viimsi, E	pot.	7	3	600	100	87.3	6.7	59.5	12.5	1.0
Pada, E	pot.	8	2	1250	50	55.4	2.7	59.4	7.9	0.4
Tartu, E	br.	14	2	1400	5	68.5	0.4	58.3	9.9	0.1
Haapsalu, E	ti.	12	1	1550	5	50.8	2.5	59.0	7.3	0.4
Tallin, E	ti.	10	1	1770	5	55.8	3.5	59.2	8.0	0.5
Nurmes, F	br.	6	3	1893	5	49.5	8.1	63.5	6.9	1.1
Rome, I	br.	-	3	110	5	66.4	4.9	41.8	11.2	0.8

6.   Discussion

The data obtained for the Finnish and Estonian collection are plotted in Fig. 8 together with the previous data available for Scandinavia, as based on the GEOMAGIA50 (*Donadini et al.,* 2006) output. The figure also shows the CALS7k model of *Korte and Constable.* (2005), as well as the data from lake sediments from Finland (*Ojala and Saarinen,* 2002; dashed dotted line in Fig. 8) and the ones form Sweden (*Snowball and Sandgren,* 2002; dashed line in Fig. 8). Fig. 9 shows an enlargement of Fig. 8, so that the data for the period AD 0-2000 are better displayed. This latter figure also shows the variation of the geomagnetic field at the Nurmijärvi magnetic observatory as calculated by *Nevanlinna* (1979) using polynomial models. The agreement between the new data, the available ones, and the model is reasonable. However, notice in particular one data (Hela97), at 670 BC, which plots far below the model estimation. A closer look at the Arai plot (Fig. 7) shows a curvature which is typical for the MD cases (*Dunlop,* 1998). In that case we used the first part of the Arai plot to determine the palaeointensity, because it produces the best statistics. However, we should mention that using a larger interval would also be possible and the data palaeointensity estimate would reduce of about 50 %. Hence, it appears that the data is not fully representative and should be treated with care.

The two figures show variable levels of agreement between the measurements and the model, However the general trend showing an increasing intensity from 5000 BC which culminates in a peak at around 500 BC can be observed. From that moment both CALS7K model and lake sediments show a gradual decrease which ends in the present day's VADM value of 7.9 10^{22} Am^2 (*Perrin and Schnepp,* 2004). The absolute

palaeointensity measurements obtained in this study are in agreement with observations of *Pesonen et al.* (1995), and show a peak around AD 500. In this sense, the result from the potteries from Viimsi (VI on Fig. 9) are in good agreement with the observations of *Pesonen et al.* (1995).
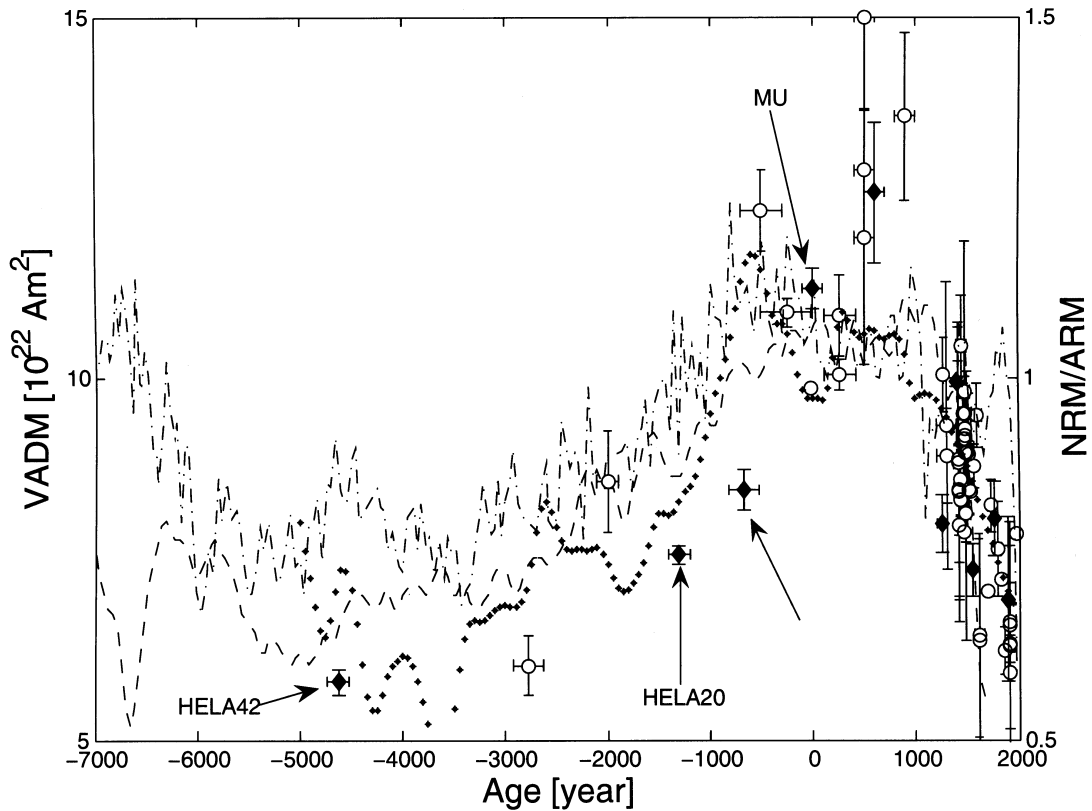

Fig. 8. Comparison of Virtual Axial Dipole Moments (VADMs) from Scandinavian samples as based on the GEOMAGIA50 database (open circles), and the new data from Finnish and Estonian specimens (closed diamonds). Stars represent the CALS7k model of *Korte and Constable* (2005) calculated at Kajaani (Central Finland; 64.2°N, 27.3°E). Dashed line and dashed-dotted line represent the lake sediment data from Sweden (*Snowball and Sandgren*, 2002), and Finland (*Ojala and Saarinen,* 2002), respectively. New results from Ylikiiminki (HELA 42, key no. 4), Kemijärvi (HELA20, key no. 3), Suomussalmi (HELA97, key no. 5), and Muskylä (MU, key no. 11) are presented.

The results of the stamped Roman bricks are displayed in terms of VADM in Fig. 10. There are a large number of available data for France and Italy between the period AD 0–500. The data appear to form a cloud with a mean VADM value of about 11 x 10^{22} Am^2. Compared to those data, the VADM value obtained from the Roman bricks appears to fit well with the higher extremity of the cloud. In particular, if we take into account the period covering AD 50–150, we obtain a mean VADM value of 10.9 ± 1.9 x 10^{22} Am^2, which is in perfect agreement with the value 11.2 ± 0.8 x 10^{22} Am^2 obtained from the bricks. The CALS7k model (*Korte and Constable,* 2005) predicts a slightly lower value at Rome (9.4 x 10^{22} Am^2).
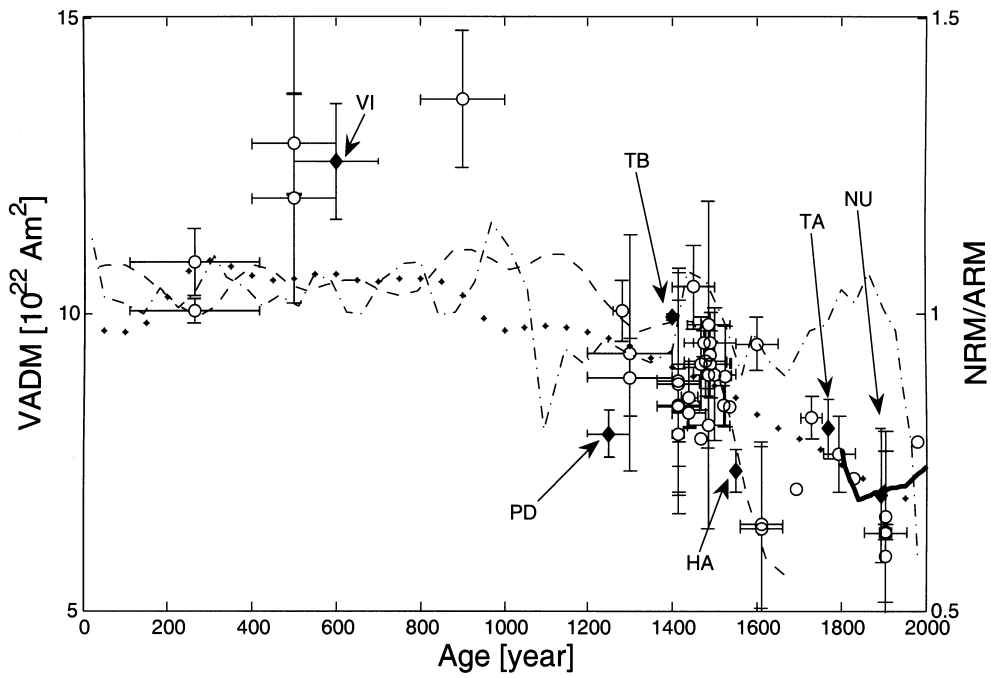
Fig. 9. Enlargement of Fig. 8 showing the last 2000 years VADM in Scandinavia. Explanations as in Fig. 8. The solid line represents the extrapolation of the VADM at the Nurmijärvi magnetic observatory (*Nevanlinna*, 1979). Results from Viimsi (VI, key no. 7), Pada (PD, key no. 8), Tartu (TB, key no. 14), Haapsalu (HA, key no. 12), Tallin (TA, key no. 10), and Nurmes (NU, key no. 6) are shown.
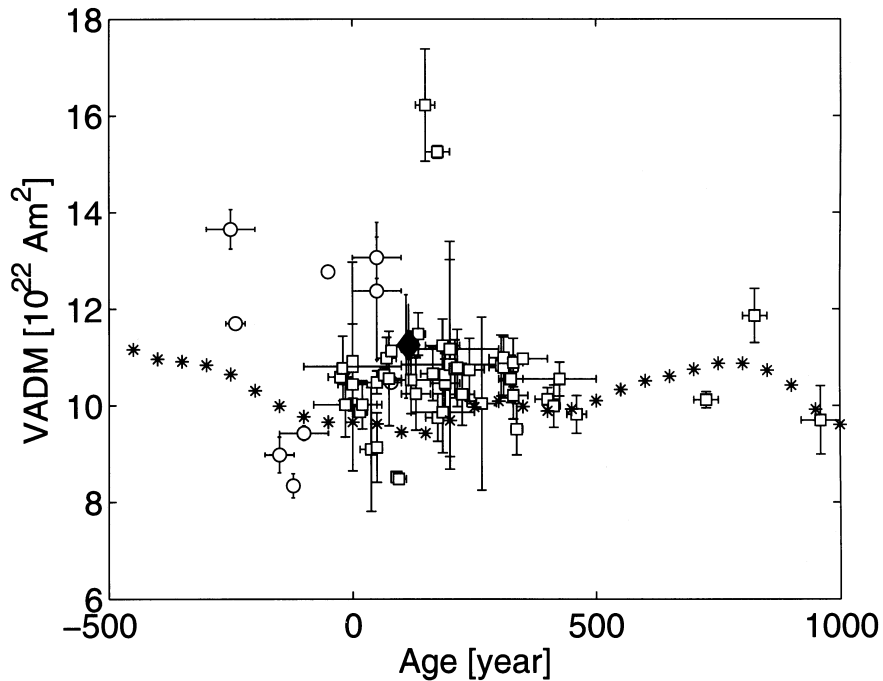

Fig. 10. Comparison of virtual axial dipole moments (VADM) from Italian (open circles) and French (open squares) samples as based on the GEOMAGIA50 database, and the measurements obtained from the stamped Roman bricks specimens (closed diamonds). Stars represent the CALS7k model of *Korte and Constable* (2005) calculated at Rome (41.8°N, 12.5°E).

7. Conclusions

This study improves the Scandinavian archaeointensity database with new reliable results. The data will be included in the GEOMAGIA50 database, and will serve for new geomagnetic field modelings.

The VADM result from the stamped Roman bricks appear to be in agreement with other data available for the period in question. In this sense, the very accurate dating of the stamps strengthens the reliability of the other results available.

References

Constable, C. and M. Korte, 2006. Is Earth's magnetic field reversing? *Earth and Planetary Science Letters*, **246 (1–2)**, 1–16.

Coe, R.S., 1967. The determination of palaeo-intensities of the Earth's magnetic field with emphasis on mechanisms which could cause non-ideal behaviour in Thellier's method. *Journal of Geomagnetism and Geoelectricity*, **19**, No 3, 157–179

Day, R., M.D. Fuller and V.A. Schmidt, 1977. Hysteresis properties of titano-magnetites: grain size and composition dependence. *Physics of the Earth and Planetary Interiors*, **13**, 260–266.

Donadini, F., K. Korhonen, P. Riisager and L.J. Pesonen, 2006. Database for Holocene geomagnetic intensity information. *EOS, Transactions, American Geophysical Union*, **87 (14)**, 137

Donadini, F., M. Kovacheva, M. Kostadinova, Ll.Casas and L.J. Pesonen, 2007. New archaeointensity results from Scandinavia and Bulgaria. Rock-magnetic studies inference and geophysical application. In preparation.

Dunlop, D.J., 1998. Thermoremanent magnetization of non uniformly magnetized grains. *Journal of Geophysical Research*, **103**, 30561–30574.

Gallet, Y., A. Genevey and F. Fluteau, 2005. Does Earth's magnetic field secular variation control centennial climate change? *Earth and Planetary Science Letters*, **236**, 339–347.

Gram-Jensen, M., N. Abrahamsen and A. Chauvin, 2000. Archaeomagnetic intensity in Denmark. *Physics and Chemistry of the Earth*, **25**, 525–531.

Hulot, G., C. Eymin, B. Langlais, M. Mandea and N. Olsen, 2002. Small-scale structure of the geodynamo inferred from the Oersted and Magsat satellite data. *Nature*, **416**, 620–623

Korte, M. and C.G. Constable, 2005. The geomagnetic dipole moment over the last 7000 years – new results from a global model. *Earth and Planetary Science Letters*, **236**, 348–358.

Nevanlinna, H., 1979. The geomagnetic field in Finland and nearby countries. *J. Geophys.*, **46**, 201–216.

Ojala, A. and T. Saarinen, 2002. Palaeosecular variation of the Earth's magnetic field during the last 10000 years based on an annually laminated sediment of Lake Nautajärvi, Central Finland. *Holocene*, **12**, 391–400.

Pesonen, L.J., M.A.H. Leino and H. Nevanlinna, 1995. Archaeomagnetic intensity in Finland during the last 6400 years: Evidence for a latitude-dependent nondipole field at ~AD 500. *Journal of Geomagnetism and Geoelectricity*, **47**, 19–40.

Perrin, M. and E. Schnepp, 2004. IAGA palaeointensity database: Distribution and quality of the data set. *Physics of the Earth and Planetary Interiors*, **147**, 255–267.

Riisager, P. and J. Riisager, 2001. Detecting multidomain magnetic grains in Thellier palaeointensity experiments. *Physics of the Earth and Planetary Interiors*, **125**, 111–117.

Riisager, P., N. Abrahamsen and J. Rytter, 2003. Research report: Magnetic investigations and the age of a medieval kiln at Kungahälla (south-west Sweden). *Archaeometry*, **45**, 665–674.

Snowball, I. and P. Sandgren, 2002. Geomagnetic field variations in northern Sweden during the Holocene quantified from varved lake sediments and their implications for cosmogenic nuclide production rates. *Holocene*, **12**, 517–530.